Highlights of Spanish Astrophysics XI, Proceedings of the XV Scientific Meeting of the Spanish Astronomical Society held on September 4–9, 2022, in La Laguna, Spain. M. Manteiga, L. Bellot, P. Benavidez, A. de Lorenzo-Cáceres, M. A. Fuente, M. J. Martínez, M. Vázquez- Acosta, C. Dafonte (eds.), 2023

Barium stars and their white-dwarf companions, a key to understanding evolved binaries.

Escorza, A.[1]

[1] European Southern Observatory, Alonso de Córdova 3107, Vitacura, Santiago, Chile
ana.escorza@eso.org

Abstract

A rich zoo of peculiar objects forms when evolved stars with extended and loosely-bound convective envelopes, such as Asymptotic Giant Branch (AGB) stars, undergo gravitational interaction in binary systems. For example, Barium (Ba) stars are main-sequence and red-giant stars that accreted mass from the outflows of a former AGB companion. This companion is now a dim and, in most cases, not directly detectable, white dwarf (WD). The orbital properties of barium stars can help us constrain interaction mechanisms in binary systems with giant components, and their chemical abundances are a tracer of the nucleosynthesis processes that took place inside the former AGB star. This contribution presents the most recent observational constraints concerning the orbital and stellar properties of Ba stars, which have increased in quantity and quality in the past few years thanks to long-term radial-velocity monitoring programs and to the accurate distances provided by the Gaia mission. However, until recently, important uncertainties affected the properties of their faint white dwarf companions, which contain key information about the formation of Ba stars. Combining radial-velocity data with Hipparcos and Gaia astrometry, we accurately measured the orbital inclinations of these binary systems and obtained the absolute masses of these otherwise hidden white dwarfs. The stellar and orbital properties of Ba stars, including the WD companion masses, are essential for our understanding of these systems and are important input parameters for binary evolution and AGB nucleosynthesis models.

1 Introduction

About half of the stars in our Galaxy are born with a companion, forming so-called binary systems. In these systems, the two components are gravitationally bound and orbit one another during their evolution. Interactions between the two stars, which can range from subtle tidal effects to common envelope evolution and mergers, including different forms of mass transfer such as wind pollution or Roche-Lobe Overflow, can have large effects on their individual evolutionary pathways. Additionally, binary interactions affect not only the fate of these orbiting stars but also the evolution of the orbital parameters of the system.

Unfortunately, many aspects of interaction physics in binaries are not yet well understood, and investigating the products that result from interacting systems is crucial to unravel the physical mechanisms involved. These statements apply to binary systems all across the Hertzsprung-Russell (HR) diagram, but here, we focus on low- and intermediate-mass systems, with components with initial masses between 1 and 5 $M_{\odot}$.

One of the prototypical families of post-interaction binaries in the mentioned mass range is Barium (Ba) stars. Ba stars are main-sequence or giant stars that show a surface enhancement of several heavy elements (including barium, which gives them their name) that should not yet be overabundant at these evolutionary stages [4]. These elements are synthesized by the slow-neutron-capture-process (s-process) of nucleosynthesis in the interior of late Asymptotic Giant Branch (AGB) stars [27]. Currently, it is widely accepted that these elements were transferred from a former AGB companion during a phase of mass transfer in the system [34]. This former AGB star, having already evolved into a cool white dwarf (WD), is currently too dim to be directly detected in most systems [44]. However, the orbital motion of the Ba star and its WD companion is detectable, and understanding the observed orbital properties of Ba-star systems, as well as the stellar properties of Ba stars and their polluters, is a key to the interaction history of these systems [24, 25].

This manuscript is mainly a summary of my Ph.D. Thesis [15], which was awarded the *Premio SEA Tesis* in 2021 and the opportunity to contribute to these proceedings. However, in order to make this contribution up to date, it also includes the part of my current work that is directly related to the thesis. The manuscript presents the most recent stellar and orbital observational constraints collected with the aim of shedding light on some of the open questions concerning Ba stars. With this purpose, we exploit the synergy between Hipparcos and Gaia data, broadband photometry, high-resolution spectroscopy, radial-velocity monitoring programs, and state-of-the-art stellar and binary evolutionary models. In Sect. 2, we describe the methodology followed to accurately locate Ba stars on the Hertzsprung-Russell (HR) diagram and determine their masses [12]. Section 3 presents the orbital properties of main-sequence and giant Ba stars [26, 13] and in Sect. 4, we present and discuss the masses of the faint WD companions [16]. In Sect. 5, we compare all these observations with binary evolution models [14] in order to investigate the evolution of these systems along the Red Giant Branch (RGB), and finally, in Sect. 6, we discuss the potential of this work and present a sample of very well-known Ba star systems that can be used to constrain binary evolution and nucleosynthesis models.

2 The HERMES-Gaia HR diagram of Barium stars

With the availability of the revolutionary parallaxes and distances provided by the Gaia mission [19, 20, 21], it is possible to construct Hertzsprung-Russell diagrams with unprecedented accuracy. Additionally, by comparing the position of stars in the HR diagram with evolutionary tracks, the evolutionary masses of single or apparently single stars can also be determined [40]. Figure 1 shows a schematic representation of the methodology used to accurately locate Ba stars on the HR diagram and determine their masses. We use a grid search method to find the MARCS atmospheric model [22] that best fits the spectral energy distribution of each

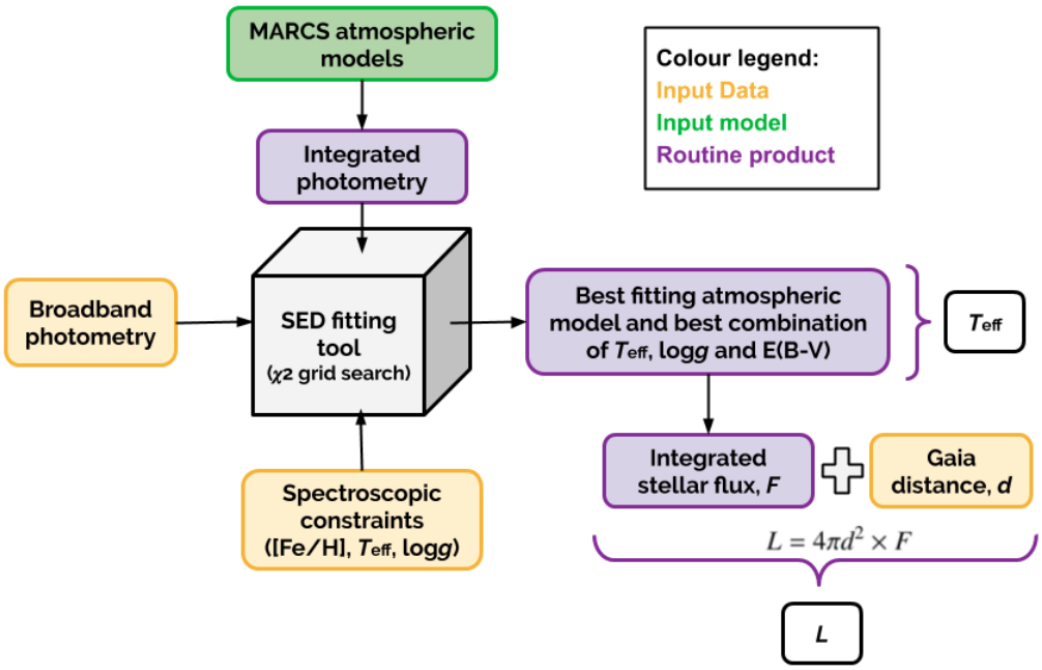

Figure 1: Schematic representation of the methodology used in [12, 13, 26, 30, 31] among others to accurately locate Ba and related stars on the Hertzsprung-Russell (HR) diagram. Broadband photometric data is compared to synthetic photometry, obtained by integrating MARCS atmospheric models [22] with the response curve of different broadband filters. Spectroscopic constraints are also considered in order to determine the best-fitting model and the line-of-sight extinction value. Finally, combining the integrated flux with the Gaia distance [2], the luminosity is derived and used together with the temperature obtained in the previous step to design an HR diagram like that of Ba stars shown in Fig. 2. Figure from [15].

star in the sample. Initially, we applied this method to over 400 Ba and related stars found in the literature and obtained some interesting mass distributions and preliminary results [12]. However, our extensive tests showed that there are important degeneracies, mainly between the temperature and the line-of-sight extinction and between the metallicity and the mass, that cannot be lifted using only broadband photometry. Because of this, at a later stage, we included constraints obtained from HERMES [37, 38] high-resolution spectra in our methodology [30, 31, 26, 13]. We showed that having independent knowledge of the metallicity is crucial, in order to use a grid of evolutionary tracks of the corresponding metallicity.

Once the best combination of stellar parameters and line-of-sight extinction is found, the stellar fluxes, integrated from the spectral energy distributions, are combined with the Gaia distances [2] to determine the accurate luminosities. We compared the location of Ba stars on the HR diagram with STAREVOL evolutionary models [41], computed for this specific sample (left panel in Fig. 2) and also determined the most probable evolutionary mass for each target, taking into account the timescale of the different evolutionary phases and

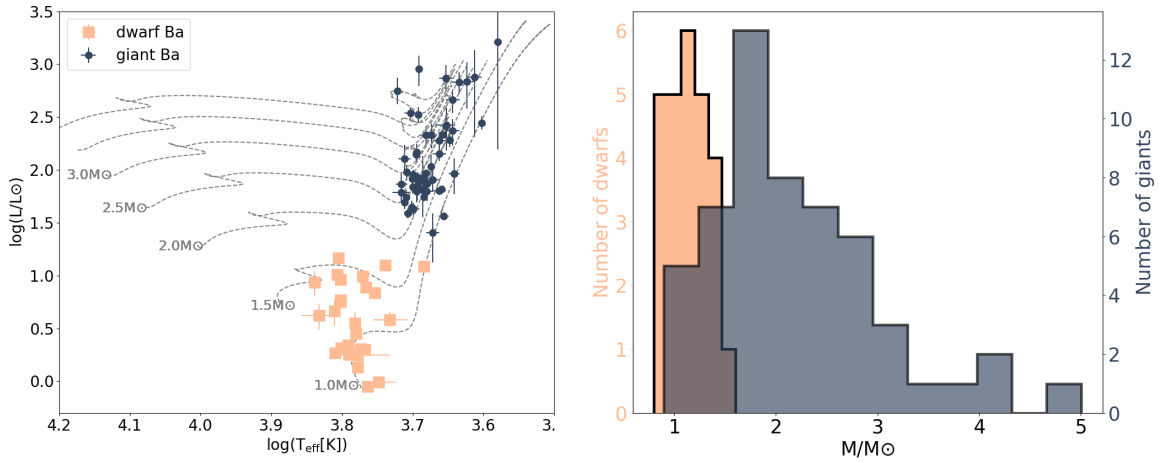

Figure 2: **Left:** Hertzsprung-Russell diagram of dwarf (squares) and giant (circles) Ba stars. STAREVOL tracks are over-plotted and used for mass determination. **Right:** Mass distribution of dwarf and giant Ba stars. Figures adapted from [13].

of tracks with different initial masses. We concluded that Ba giants have masses from 1 to 5 $M_{\odot}$, with their mass distribution peaking around 2 $M_{\odot}$, while main-sequence Ba stars cover a much narrower mass range than their giant counterparts, from 0.9 to 1.6 $M_{\odot}$ (right panel in Fig. 2), opening questions about the observational biases against hotter main-sequence polluted objects. Additionally, the deficit of low-mass barium giants was associated to binary interaction between the evolving Ba star and its WD companion, given the fact that low-mass stars reach large radii at the tip of the red giant branch. This was investigated by [14] and it is discussed in Sect. 5.

3 The $e \log P$ diagram of Barium stars

Giant Ba stars have been intensively investigated since their discovery, but main-sequence Ba stars were discovered later and are much less sampled and studied than their giant counterparts [35]. Since the polluting episode is expected to happen when the Ba star is still in the main-sequence phase [25], the properties of these systems are essential to have a complete picture of the formation and evolution of Ba stars. Recently, we presented the largest systematic study of the orbital properties of main-sequence Ba stars and a thorough comparison of these properties to those of the Ba giants [13]. This work was based on radial-velocity data. We combined recent radial-velocity measurements from HERMES [37, 38] and SALT-HRS [5, 9] high-resolution spectra with archival radial-velocity data from CORAVEL [3].

Fig. 3 shows the two main orbital parameters, the period and the eccentricity, of main-sequence and giant Ba stars in an eccentricity-period diagram or $e \log P$ diagram. Main-sequence Ba stars show orbital periods between 200 and 11 000 days and eccentricities over the whole range from 0 to over 0.8, similar to Ba giants. We note that the observational

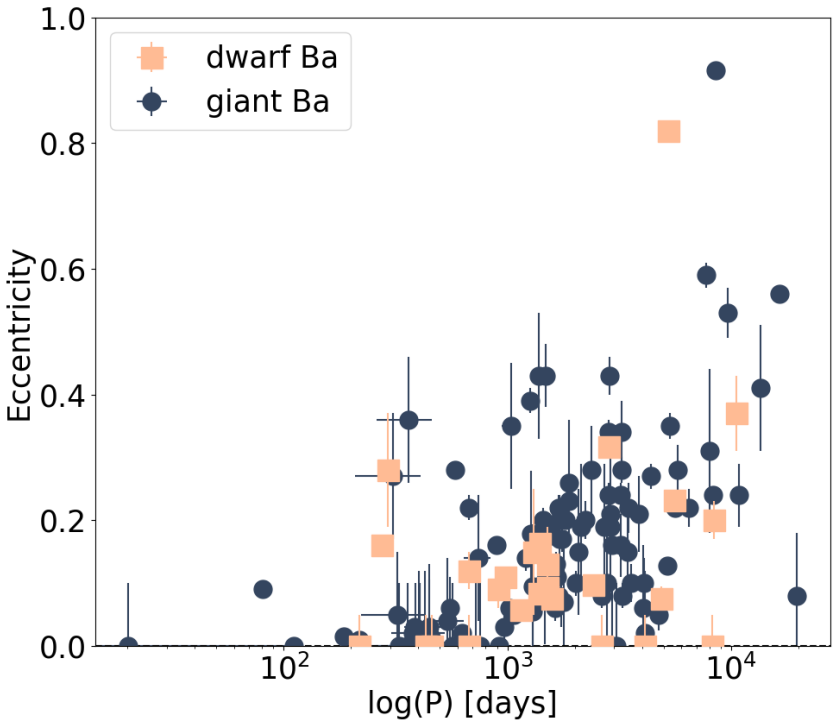

Figure 3: $e \log P$ diagram of dwarf (squares) and giant (circles) Ba stars. Figure adapted from [13].

effort behind Fig. 3 is enormous, and that some of these systems have been part of multi-decade radial-velocity monitoring programs with different instruments, especially with the CORAVEL spectrometers and the HERMES spectrograph.

The orbital properties of Ba stars are not well understood [36]. Binary evolution and interaction models predict that systems with periods below 3000–5000 days should have negligible eccentricities after interacting with an AGB star [23]. However, the region of the $e \log P$ diagram occupied by Ba stars is also populated by several other families of post-mass-transfer evolved binaries, making this figure one of the biggest unresolved puzzles concerning evolved low- and intermediate-mass binaries.

4 The masses of the white dwarf companions

As mentioned above, the white dwarf companions of Ba stars are dim, cool, and difficult to observe via direct methods. However, they contain key information about binary interaction processes, about the s-process of nucleosynthesis, and about the formation of Ba stars. Recently, we combined the radial-velocity data used to determine the orbits presented in Fig. 3 with Hipparcos and Gaia astrometry and with the Hipparcos-Gaia catalogue of accelerations (HGCA; [6, 7]) in order to use the dynamical information of these systems to determine the

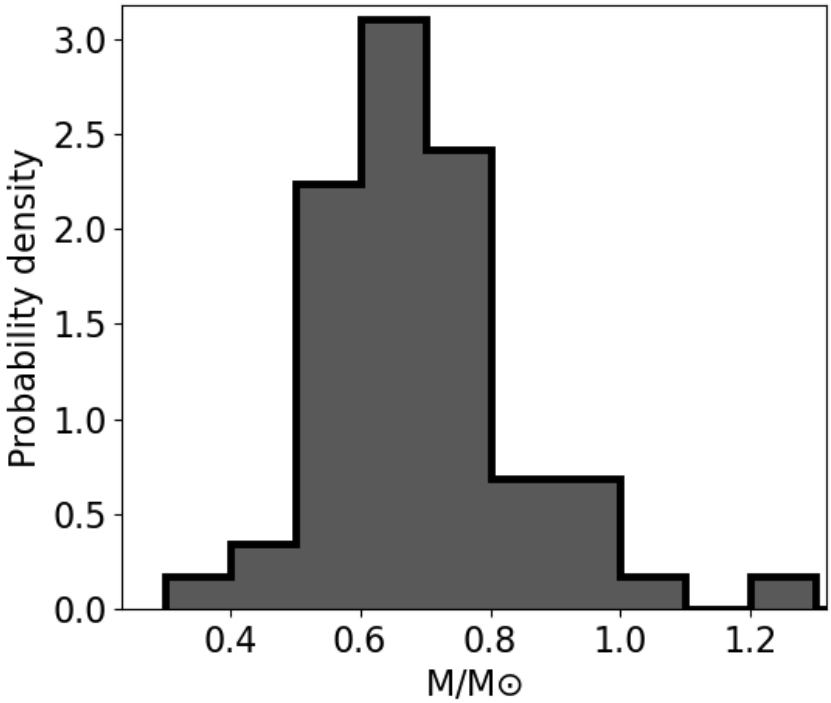

Figure 4: Mass distribution of the WD companions of Ba star. Data from [16]

masses of the faint companions. We used the software package ORVARA [8], designed to simultaneously fit a single Keplerian model to any combination of radial-velocity and astrometric data using a parallel-tempering Markov chain Monte Carlo method. Adopting Gaussian priors for the Ba star masses (obtained as described in Sect. 2) and for the parallaxes (from Gaia EDR3 [21] or from the Gaia DR3 non-single-star catalogue [18] when available), and assuming uninformative priors for the orbital elements and the WD masses, we determined new orbital inclinations and companion masses for 60 Ba star systems. This combination of data allowed us to constrain new orbits and improve the orbits for the longest-period systems. Additionally, we unravelled a new triple system that was not known before (HD 218356) and constrained the orbits and the masses of the two companions, and we discovered a neutron star candidate accompanying a thought-to-be Ba star that is probably a normal giant (56 UMa, [17]).

Figure 4 shows the WD mass distribution obtained. The weighted average is slightly more massive than that of field WDs, and there is an excess of WDs with masses higher than 0.7 - 0.8 $M_{\odot}$ considering the 1σ uncertainties. This indicates that they might come from AGB stars that are more massive than 3 $M_{\odot}$ [33], and these AGB stars would be more massive than what the abundance ratios on Ba star atmospheres and theoretical models of the s-process of nucleosynthesis seem to expect [32, 30, 10].

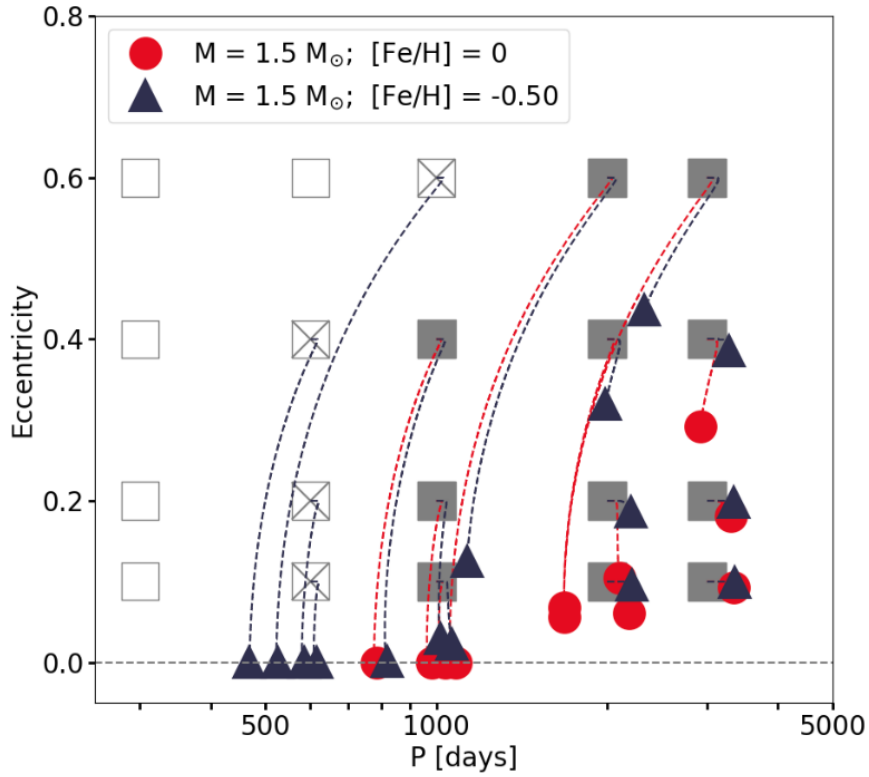

Figure 5: Evolution of the period and the eccentricity of binary systems formed by a main-sequence Ba star of 1.5 $M_\odot$ with solar (red circles) or subsolar (blue triangles) metallicity. The squares represent the initial orbital elements, the lines show the evolution of these elements as the Ba star evolves along the red-giant branch, and the coloured symbols show the orbital parameters at the moment of He-core ignition. Empty squares indicate systems that merge at both metallicities due to binary interaction. Those with a cross only merge at solar metallicity, and the systems with shaded squares reach core-He burning stage at both metallicities. Figure from [14].

5 The evolution of Ba stars along the Red Giant Branch

The distributions of masses, periods, and eccentricities presented above provide strong constraints to theoretical studies. Here, we focus on the comparison between main-sequence and giant Ba stars, which allows us to investigate the evolution of the binary orbit between these two phases [14]. Our detailed binary evolution models, computed with the BINSTAR code [42, 11], showed that a second stage of binary interaction, this time between the main-sequence Ba star and its WD companion, also takes place in some of these systems, affecting the distribution of orbits and masses observed among Ba giants. Our models suggest that main-sequence Ba stars of less than 2 $M_\odot$ in systems with periods below 500 to 1000 days (depending on mass and metallicity) will merge with their WD companions and never become core-He-burning giants. As an example, Fig. 5 shows the evolution, on an eccentricity-period

Table 1: List of Ba stars with well-constrained orbital parameters (we list here the period, the eccentricity, the semimajor axis, and the inclination and refer to [26, 13, 16] for the remaining parameters), Ba star and WD masses, and recently determined chemical abundances from high-resolution spectra.

Star ID	P [days]	e	a [AU]	i [°]	$M_{\rm Ba}$	$M_{\rm WD}$	Abund.
BD-14°2678	3481 ± 205	0.25 ± 0.05	7.0 ± 0.5	93 ± 18	3.0 ± 0.2	0.67 ± 0.10	[39]
HD 5424	1906 ± 17	0.19 ± 0.05	3.7 ± 0.4	30 ± 3	1.3 ± 0.4	0.52 ± 0.11	[30, 39]
HD 16458	2017 ± 15	0.10 ± 0.03	4.2 ± 0.5	61 ± 12	1.90 ± 0.10	0.74 ± 0.15	[30]
HD 20394	2248 ± 8	0.16 ± 0.06	4.6 ± 0.5	31 ± 3	2.0 ± 0.2	0.49 ± 0.1	[39]
HD 27271	1681.1 ± 1.0	0.224 ± 0.007	4.2 ± 0.3	103 ± 5	2.9 ± 0.2	0.70 ± 0.09	[30]
HD 40430	6147 ± 278	0.26 ± 0.02	9.4 ± 0.8	23.4 ± 0.6	2.3 ± 0.2	0.7 ± 0.12	[39]
HD 43389	1688.4 ± 1.4	0.083 ± 0.017	4.0 ± 0.7	111 ± 3	1.8 ± 0.4	0.76 ± 0.25	[30, 39]
HD 49841	897.5 ± 1.9	0.162 ± 0.015	2.8 ± 0.1	109 ± 19	2.85 ± 0.10	0.82 ± 0.16	[39]
HD 50082	2883 ± 6	0.19 ± 0.02	5.1 ± 0.9	63 ± 3	1.6 ± 0.3	0.56 ± 0.18	[30]
HD 51959	11195 ± 475	0.30 ± 0.05	11.8 ± 1.0	163.2 ± 0.8	1.2 ± 0.1	0.51 ± 0.08	[39]
HD 53199	8233 ± 175	0.255 ± 0.010	11.7 ± 0.5	103 ± 7	2.5 ± 0.1	0.64 ± 0.05	[39]
HD 58121	1217 ± 5	0.135 ± 0.019	3.4 ± 0.5	121 ± 4	2.6 ± 0.5	0.67 ± 0.19	[39]
HD 59852	3477 ± 80	0.14 ± 0.08	6.6 ± 0.8	26 ± 4	2.5 ± 0.3	0.62 ± 0.15	[39]
HD 87080	274.31 ± 0.05	0.162 ± 0.016	1.05 ± 0.10	60 ± 12	1.38 ± 0.15	0.70 ± 0.18	[1]
HD 88562	1451.0 ± 1.0	0.203 ± 0.013	2.9 ± 0.3	87 ± 9	1.0 ± 0.1	0.48 ± 0.09	[30, 39]
HD 91208	1770 ± 3	0.178 ± 0.018	4.2 ± 0.4	134 ± 2	2.3 ± 0.2	0.83 ± 0.14	[39]
HD 95193	1652 ± 5	0.13 ± 0.02	4.12 ± 0.15	81 ± 25	2.7 ± 0.1	0.71 ± 0.08	[39]
HD 104979	18518 ± 1205	0.12 ± 0.04	21.1 ± 1.7	147.8 ± 1.6	2.7 ± 0.2	0.94 ± 0.14	[29]
HD 107541	3583 ± 47	0.09 ± 0.04	5.5 ± 0.8	128 ± 3	1.1 ± 0.2	0.55 ± 0.16	[39]
HD 107574	1384.8 ± 1.5	0.083 ± 0.005	2.99 ± 0.12	166.3 ± 0.4	1.11 ± 0.05	0.74 ± 0.06	[29]
HD 119185	25385 ± 5114	0.61 ± 0.08	23 ± 3	98 ± 13	1.7 ± 0.2	0.65 ± 0.08	[39]
HD 123949	8544 ± 12	0.9167 ± 0.0007	10.8 ± 0.9	122 ± 72	1.3 ± 0.3	0.78 ± 0.15	[30, 39]
HD 139195	5296 ± 14	0.32 ± 0.02	8.8 ± 0.3	97.6 ± 1.1	2.6 ± 0.1	0.66 ± 0.05	[43]
HD 143899	1461.8 ± 1.2	0.18 ± 0.04	3.66 ± 0.15	124.6 ± 2.5	2.4 ± 0.1	0.66 ± 0.06	[39]
HD 178717	2912 ± 14	0.46 ± 0.03	5.2 ± 0.8	35 ± 4	1.6 ± 0.9	0.53 ± 0.16	[30]
HD 180622	4045 ± 30	0.08 ± 0.04	6.9 ± 1.2	100 ± 6	1.8 ± 0.3	0.80 ± 0.25	[39]
HD 183915	4344 ± 20	0.41 ± 0.04	7.1 ± 1.2	174.3 ± 0.3	1.8 ± 1.0	0.61 ± 0.19	[39]
HD 200063	1743 ± 8	0.07 ± 0.04	4.3 ± 0.5	115 ± 5	2.0 ± 1.3	0.95 ± 0.26	[39]
HD 201824	2922 ± 23	0.30 ± 0.04	5.5 ± 1.1	59 ± 66	1.7 ± 0.4	0.78 ± 0.28	[39]
HD 204075	2367 ± 9	0.26 ± 0.05	6.0 ± 0.4	133 ± 5	4.5 ± 0.3	0.67 ± 0.10	[43, 39]
HD 205011	2846 ± 5	0.23 ± 0.02	5.3 ± 0.9	74 ± 5	1.8 ± 0.3	0.61 ± 0.19	[43]
HD 210946	1521 ± 0.9	0.109 ± 0.011	3.9 ± 0.5	114 ± 8	1.8 ± 0.5	0.86 ± 0.26	[39]
HD 216219	3948 ± 23	0.09 ± 0.05	6.2 ± 0.4	33.5 ± 1.8	1.45 ± 0.10	0.63 ± 0.08	[28]

diagram, of two grids of 20 models each. All the systems modelled for this plot start their evolution with a main-sequence Ba star of 1.5 $M_\odot$ and a WD companion. The grid plotted in red corresponds to systems with solar metallicity, while the dark blue one shows systems with sub-solar metallicity. The squares represent the initial orbital elements of the modelled binary systems when the Ba star was a main-sequence star. The lines show the evolution of these elements along the giant branch of the Ba star, and the coloured symbols show the final orbital parameters at the onset of He-core burning. We show that depending on the metallicity, the Ba stars in many of these systems (those without a corresponding final symbol) will never ignite their helium cores. As mentioned before, we concluded that even though we observe such Ba star systems in the main-sequence phase, these systems will likely merge and not become part of the Ba giant population.

6 Conclusions and discussion

Despite the efforts to describe the properties and evolution of Ba stars, further research is necessary to entirely understand their formation and evolution. From the observational side, identifying main-sequence Ba stars with higher masses is needed to complete the full evolutionary picture. Additionally, larger samples should be built, making use of large spectroscopic surveys. Of course, further theoretical research is also necessary. The orbital properties of this family of post-interaction binary systems cannot be properly explained yet, and the exact mass-transfer mechanism responsible for the pollution of Ba stars is not well-defined. In any case, the observational constraints presented in [15] and in this contribution are important for future investigation of interaction mechanisms in low- and intermediate-mass binary systems as well as of AGB nucleosynthesis models. To help with this purpose, we have collected in Table 1 a sample of well-known Ba stars that can be used to constrain the mentioned models. The table only includes systems with well-constrained orbits, masses available for both the Ba star and the WD, and stellar parameters and individual abundances determined from high-resolution high signal-to-noise spectra. The table lists their main orbital parameters (period P, eccentricity e, semimajor axis a, and inclination i) determined as described in Sects. 3 and 4, the Ba star masses determined as described in Sect. 2, and the WD masses determined as described in Sect. 4. In order to ensure the quality of the orbital inclinations and the WD masses, we only included systems with a significant orbital acceleration in the HGCA (see [16] for more details). Since the work summarized here did not focus on the chemistry of Ba stars, we list in the last column of the table recent references where the individual chemical abundances of several elements, including s-process elements, were determined from high-quality spectra.

These are exceptional times for stellar and binary evolution research. New telescopes, instruments, surveys, and theories keep coming, providing new pieces to solve this and many other puzzles. Low- and intermediate-mass stars are very common, and they are major contributors of carbon, nitrogen, many heavy elements, and dust to their host galaxies, and since at least half of them evolve in binary systems, nucleosynthesis and interaction physics are essential to our understanding of stellar evolution and the chemical evolution of galaxies.

Acknowledgments

The author wants to thank the Spanish Astronomy Society for awarding their 2021 Thesis Prize to the work summarized in this contribution. The PhD Thesis was mainly funded by the Fonds voor Wetenschappelijk Onderzoek Vlaanderen (FWO) under contract ZKD1501-00-W01 and by the Belgian Science Policy Office under contract BR/143/A2/STARLAB for the first year. The HERMES spectrograph is supported by the Fund for Scientific Research of Flanders (FWO), the Research Council of KU Leuven, Belgium, the Fonds National de la Recherche Scientifique (F.R.S.-FNRS), the Royal Observatory of Belgium, the Observatoire de Genève, and the Thüringer Landessternwarte Tautenburg. This work has made use of data from the European Space Agency (ESA) mission Gaia processed by the Gaia Data Processing and Analysis Consortium (DPAC). Funding for the DPAC has been provided by national institutions, in particular the institutions participating in the Gaia Multilateral Agreement. This research has also made use of the SIMBAD database, operated at CDS,

Strasbourg, France.

References

[1] Allen, D. M. & Barbuy, B. 2006, A&A, 454, 895

[2] Bailer-Jones, C. A. L., Rybizki, J., Fouesneau, M., et al. 2018, ApJ, 156, 58

[3] Baranne, A., Mayor, M., & Poncet, J. L. 1979, Vistas Astron., 23, 279

[4] Bidelman, W. P. & Keenan, P. C. 1951, ApJ, 114, 473

[5] Bramall, D. G., Sharples, R., Tyas, L., et al. 2010, Proc. SPIE, 7735, 77354F

[6] Brandt, T. D. 2018, ApJS, 239, 31

[7] Brandt, T. D. 2021, ApJS, 254, 42

[8] Brandt, T. D., Dupuy, T. J., Li, Y., et al. 2021, AJ, 162, 186

[9] Crause, L. A., Sharples, R. M., Bramall, D. G., et al. 2014, Proc. SPIE, 9147, 91476T

[10] Cseh, B., Lugaro, M., D'Orazi, V., et al. 2018, A&A, 620, A146

[11] Davis, P. J., Siess, L., & Deschamps, R. 2013, A&A, 556, A4

[12] Escorza, A., Boffin, H. M. J., Jorissen, A., et al. 2017, A&A, 608, A100

[13] Escorza, A., Karinkuzhi, D., Jorissen, A., et al. 2019, A&A, 626, A128

[14] Escorza, A., Siess, L., Van Winckel, H., & Jorissen, A. 2020, A&A, 639, A24

[15] Escorza, A. 2020, PhD thesis, KU Leuven and Université Libre de Bruxelles

[16] Escorza, A. & De Rosa, R. J. 2023, arXiv e-prints, arXiv:2301.04232

[17] Escorza, A., Karinkuzhi, D., Jorissen, A., et al. 2023, A&AL, accepted.

[18] Gaia Collaboration, Arenou, F., Babusiaux, C., et al. 2022, arXiv e-prints, arXiv:2206.05595

[19] Gaia Collaboration, Brown, A. G. A., Vallenari, A., et al. 2018, A&A, 616, A1

[20] Gaia Collaboration, Brown, A. G. A., Vallenari, A., et al. 2021, A&A, 649, A1

[21] Gaia Collaboration, Brown, A. G. A., Vallenari, A., et al. 2016, A&A, 595, A1

[22] Gustafsson, B., Edvardsson, B., Eriksson, K., et al. 2008, A&A, 486, 951

[23] Izzard, R. G., Dermine, T., & Church, R. P. 2010, A&A, 523, A10

[24] Jorissen, A., Van Eck, S., Mayor, M., & Udry, S. 1998, A&A, 332, 877

[25] Jorissen, A. 2004, in Asymptotic Giant Branch Stars. Springer, 2004., 461–518

[26] Jorissen, A., Boffin, H. M. J., Karinkuzhi, D., et al. 2019, A&A, 626, A127

[27] Käppeler, F., Gallino, R., Bisterzo, S., & Aoki, W. 2011, Reviews of Modern Physics, 83, 157

[28] Karinkuzhi D., Goswami A., 2014, MNRAS, 440, 1095

[29] Karinkuzhi, D. & Goswami, A. 2015, MNRAS, 446, 2348

[30] Karinkuzhi, D., Van Eck, S., Jorissen, A., et al. 2018, A&A, 618, A32

[31] Karinkuzhi, D., Van Eck, S., Goriely, S., et al. 2021, A&A, 645, A61

[32] Lugaro, M., Karakas, A. I., Stancliffe, R. J., & Rijs, C. 2012, ApJ, 747, 2

[33] Marigo, P., Bossini, D., Trabucchi, M., et al. 2022, ApJS, 258, 43

[34] McClure, R. D. 1984, ApJ, 280, L31

[35] North, P., Jorissen, A., & Mayor, M. 2000, in IAU Symposium, Vol. 177, 269

[36] Pols, O. R., Karakas, A. I., Lattanzio, J. C., & Tout, C. A. 2003, in Astronomical Society of the Pacific Conference Series, Vol. 303

[37] Raskin, G., van Winckel, H., Hensberge, H., et al. 2011, A&A, 526, A69

[38] Raskin, G., van Winckel, H., Hensberge, H., et al. 2011, A&A, 526, A69

[39] Roriz, M. P., Lugaro, M., Pereira, C. B., et al. 2021, MNRAS, 507, 1956

[40] Serenelli, A., Weiss, A., Aerts, C., et al. 2021, A&ARv, 29, 4

[41] Siess, L. 2006, A&A, 448, 717

[42] Siess, L., Izzard, R. G., Davis, P. J., & Deschamps, R. 2013, A&A, 550, A100

[43] Smiljanic R., Porto de Mello G. F., da Silva L., 2007, A&A, 468, 679

[44] Webbink, R. F. 1986, Highlights of Astronomy, 7, 185